MULTIPLICITY AND DISORDER IN THE LATTICE OF EKMANITE

BARTHOLOMEW NAGY,* *Pennsylvania State University, State College, Pennsylvania.*

ABSTRACT

Chemical evidence indicates that ekmanite, a flaky hydrous-iron-manganese silicate mineral, is related to the layer lattice silicates. The results of single crystal *x*-ray studies suggest that ekmanite possesses a structure that is essentially a packing of talc-type sheets and interleaved cations and that the orthohexagonal cell is a multiple of a sub-unit of the following dimensions: $a=5.54$ Å, $b=9.60$ Å, and $c=12.08$ Å. The distribution of diffuse reflections indicates the presence of a disordered lattice related to random and *irregular* shifts of the talc-type units.

An *x*-ray investigation was undertaken in an attempt to determine the mineralogical position of ekmanite. It is expected that the study of rare, hydrous-silicate minerals like ekmanite may result in data that can be significant with respect to the entire layer lattice silicate group.

Ekmanite was first described from its occurrence at Grythytte, Sweden, by Igelström, as reported by Dana (1892). It was found to be a flaky, massive or asbestiform mineral that has a color varying between light green and black, and resembles the common types of chlorites in its megascopic appearance. Ekmanite was reported to be associated with the magnetite iron ore.

Jakob (1923) reexamined ekmanite samples from the same locality and came to the conclusion that the mineral is related to the friedelite-pyrosmalite group. Jakob emphasized the fact that the ekmanite crystals very commonly show perfect basal cleavage planes, and noted that the mineral is apparently optically uniaxial. This agrees with the results of Hamberg, as reported by Dana, who also concluded that ekmanite is uniaxial. This conclusion was confirmed by the results of the optical investigation performed during the present study.

INVESTIGATION OF THE CHEMICAL RELATIONSHIP BETWEEN EKMANITE AND THE LAYER LATTICE SILICATES

Chemical analyses of ekmanite obtained from the literature and differential thermal analysis curves prepared during the present study were compared with those of known sheet structure minerals and it was concluded that the available data seemed to suggest the existence of a chemical relationship between ekmanite and the layer lattice silicates.

There are only a few chemical analyses available of ekmanite. The chemical data show that this mineral is essentially an iron-manganese

---

* Present address: Stanolind Oil and Gas Company, P.O. Box 591, Tulsa 2, Oklahoma.

hydrous-silicate that usually also contains a small percentage of alumina and magnesia. Table 1 shows seven chemical analyses of ekmanite; the first six of these analyses were given by Igelström and the seventh by Jakob; Igelström's analyses were obtained from Dana. A chemical analysis of stilpnomelane was also included in Table 1, in order to enable one to compare the chemical composition of this mineral with the chemical data of ekmanite.

TABLE 1. CHEMICAL ANALYSES OF EKMANITE AND STILPNOMELANE

	Ekmanite							*Stilpnomelane*
	1	2	3	4	5	6	7	8
SiO_2	34.30	36.42	40.30	37.07	37.69	36.82	39.41	45.61
Al_2O_3	tr	1.07	5.08	5.85	—	3.63	8.36	5.00
Fe_2O_3	4.97	4.79	3.60	—	—	—	14.06	—
FeO	35.78	24.27	25.54	38.20	36.07	31.09	13.54	37.70
MnO	11.45	21.56	7.13	6.32	14.74	9.29	5.15	—
MgO	2.99	tr	7.64			7.53	3.69	3.00
CaO	—	tr	—	2.73	—	tr	4.51	—
H_2O	10.51	9.91	10.74	9.71	11.50	10.71	9.42	9.14
CO_2	—	—	—	—	—	—	1.94	—
	100.00	98.02	100.03	99.88	100.00	99.07	100.08	100.45

Analyses 1–6 and 8 were reported by Igelström and listed by Dana (1892).
Analysis 7 was given by Jakob (1923).

An approximate chemical formula was calculated from the average of these seven analyses. It may be written in the following oxide form:

$$(Fe, Mn, Mg)\,O \cdot SiO_2 \cdot H_2O.$$

The molecular ratio between silica and the oxides of the other cations is approximately 1:1. An arbitrary step was taken during the calculations that consisted of grouping the silica and alumina together, and including ferric iron in the total sum of the ferrous, manganese and magnesium oxides. Due to the relatively low amounts of alumina and ferric iron present in most of the chemical analyses, the fundamental 1:1 ratio between silica and the metallic oxides does not appear to be seriously affected even if a different grouping of the oxides were to be chosen.

The chemical composition of ekmanite was compared with that of other hydrous silicate minerals. The ratio between the silicon ion and the other cations present in ekmanite is approximately the same as in biotite. It is lower than that of talc, stilpnomelane and also tremolite, but it is higher than the ratio present in chrysotile and chlorite.

Another approach that was followed during the investigation of the relationship between ekmanite and other hydrated silicate minerals involved the comparison of the differential thermal analysis curves. The *DTA* patterns of ekmanite are characterized by a double exothermic peak between approximately 250–450° C. and another weaker exothermic reaction at approximately 770° C. There is only one endothermic peak present on the differential thermal analysis patterns; this peak occurs around 140° C.

The ekmanite *DTA* curves resemble those of stilpnomelane. In Fig. 1 an ekmanite differential thermal analysis pattern is shown together with that of a mineral that appeared to be stilpnomelane and one of clinochlore. All of the *DTA* runs were made at the heating rate of 600° C. per hour, using platinum crucible sample holders and a continuously recording potentiometer unit. The differential thermal analysis patterns were recorded on a chart on which one set of coordinates were curved lines. The patterns were replotted, however, on a rectangular coordinate system in order to facilitate their observation. Furthermore, it was also thought that it might be easier to compare these re-plotted curves with the *DTA* patterns of other hydrous silicates present in the literature which are usually plotted on rectangular coordinate system.

The high temperature endothermic reaction that occurs with clay minerals was absent on the ekmanite differential thermal analysis patterns. One of the *DTA* runs performed on stilpnomelane showed an endothermic peak at approximately 660° C., but it was impossible to reproduce this peak. The *DTA* curve of stilpnomelane shown in Fig. 1 represents a pattern which seemed to be characteristic and reproducible. Gruner (1937) reported that stilpnomelane loses water around 500° C.; this temperature, however, is very close to the upper limit of the temperature at which the exothermic reaction occurs. Hutton (1938) reported that this water loss of stilpnomelane occurs around 350° C. This temperature coincides with the temperature of the exothermic reaction caused by the oxidation of ferrous iron and consequently the development of the strong exothermic peak of the differential thermal analysis patterns may interfere with the development of an endothermic peak.

The exothermic peaks present on the ekmanite and stilpnomelane *DTA* patterns below 500° C. may be due to the oxidation of the ferrous iron. This possibility is based on the results of experiments performed with ferrous and sodium oxalate. These two (chemically pure) materials were run in the differential thermal analysis unit in order to note the approximate temperature at which the exothermic reaction due to the oxidation of the ferrous iron takes place. The differential thermal analysis of sodium oxalate served as a control on the ferrous oxalate run; if the exothermic

FIG. 1. Differential thermal analysis patterns of (*A*) ekmanite, (*B*) stilpnomelane, (*C*) clinochlore, (*D*) ferrous oxalate and (*E*) sodium oxalate.

reaction in question were not caused by the oxidation of ferrous iron, one might expect it to occur in both ferrous and sodium oxalate *DTA* patterns. The differential thermal analysis curves of ferrous and sodium oxalate are shown in Fig. 1. The exothermic reaction between approximately 300 and 500° C. occurred only in the case of ferrous oxalate. This strengthens the possibility that the similar reactions which occurred during the heating of ekmanite and stilpnomelane might also be caused by the oxidation of ferrous iron. These reactions, however, may not be due entirely to the oxidation of ferrous iron but may also be the result of the oxidation of manganese that is expected to occur in the same temperature range. One may draw an analogy between the exothermic reactions of ekmanite or stilpnomelane and ferrous oxalate only if the bond strengths between the ferrous iron and the surrounding ions are similar in both materials. Such a relationship is anticipated due to the fact that in the stilpnomelane structure (Gruner, 1944) iron is located between the talc-type layers and between the Si-O double sheets.

According to Gruner the crystal structure of stilpnomelane consists of a talc-type unit together with ions located between the basal planes of this unit. Although the chemical composition of ekmanite is somewhat different from that of stilpnomelane, *x*-ray investigations showed that the two minerals may be closely related.

Single Crystal *X*-ray Investigation of Ekmanite

In order to determine the cell dimensions and symmetry of ekmanite Laue photographs, rotation, oscillation, Weissenberg diagrams and powder patterns were taken. The material employed was obtained from a specimen from Brunsjö (near Grythytte), Sweden; some of the flakes present in this sample were large enough for single crystal *x*-ray studies. Because of the presence of a greenish-gray coating that often covered the particles, the sample was examined under a binocular microscope in order to detect the presence of any visible impurity and in order to be able to discard all impure flakes. The flakes selected for the single crystal *x*-ray studies showed excellent basal cleavage planes. Poor development of the crystals around the edges prevented the appearance of other faces, with the exception of a distorted, apparently pyramidal face that was present on some of the particles.

Unfiltered molybdenum radiation was used for the Laue diagrams. The Weissenberg photographs were taken with iron and the rotation diagrams with both iron and molybdenum radiation. Iron radiation proved to be a suitable choice for the last two methods because of the ferriferous nature of ekmanite and the large cell dimensions.

The Laue photographs taken normal to the basal plane show both diffuse streaks and spots. Those spots which do not lie along the strong, diffuse streaks may be connected with very weak streaks. A three-fold axis was detected normal to the basal plane together with three vertical mirror planes intersecting each other at the center of the diagram at 120° angles. These features can be seen on Fig. 2 which is a reproduction of a Laue diagram taken with the *x*-ray beam normal to the basal plane. The symmetry elements present on the photographs indicate that the Laue symmetry of ekmanite is D_{3h}.

The first rotation diagrams were taken with Mo radiation and the photographs were exposed for twelve hours. Photographs taken by rotating the crystal about an axis which was later found to be the orthohexagonal *b* axis show five well developed layer lines together with a few very weak and diffuse spots at approximately 1/3 and 2/3 height between the zero and what appeared to be the first layer line. The identity period between the zero and the first layer lines was found to be 3.2 Å; such a value is low by analogy with other chemically similar minerals. In order to detect the true identity period between the zero and the first layer lines the rotation diagrams were retaken with FeK_α radiation and an exposure of 48 hours. The resultant photograph reveals a different periodicity. The identity period appears to be much larger than the previously observed value; it was found to be 38.40 Å and the strong line at 3.2 Å position is preceded by 11 more layer lines. The rotation diagrams are characterized by the strong 0 and 12th layers and by the large number of closely spaced, comparatively weak reflections of the intermediate layer lines. Most of the reflections appear to be diffuse streaks rather than sharp spots. It is important to note that "streaky" reflections are present on all of the layer lines; and since the rotation axis is the orthohexagonal *b* axis, one may conclude that such reflections are not restricted to planes

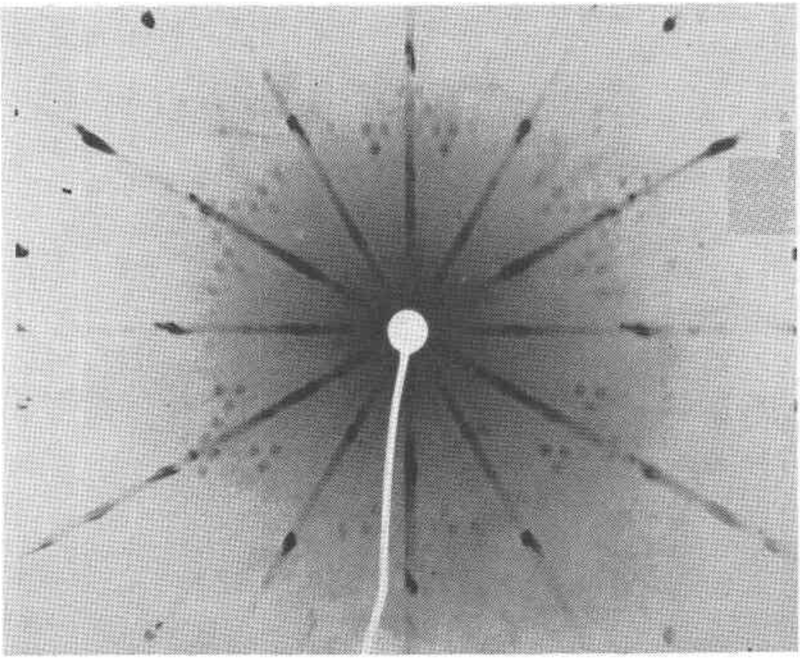

FIG. 2. Laue photograph of ekmanite taken with the *x*-ray beam normal to the basal plane. Unfiltered Mo radiation.

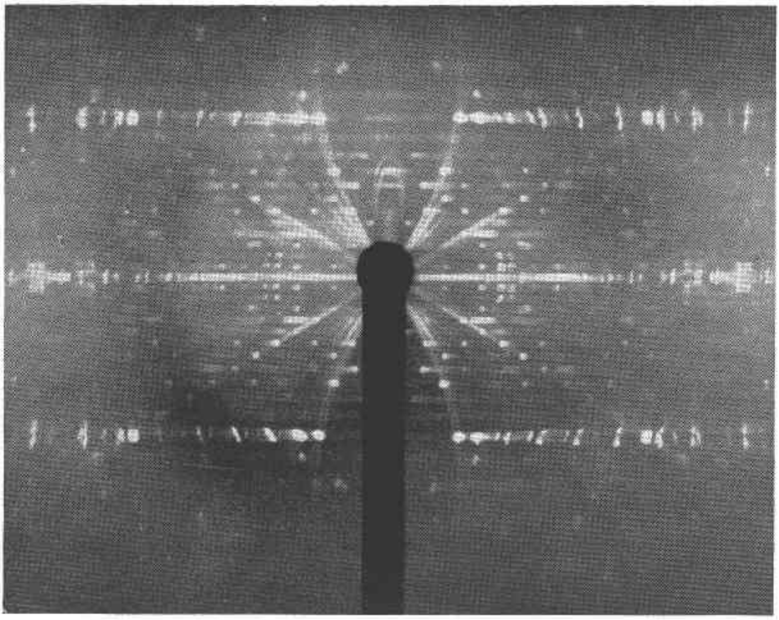

FIG. 3. Rotation diagram of ekmanite taken with rotation around the *b* axis. Fe K_α radiation. Most of the weak, diffuse reflections were lost when a reversed (negative) print was made from the original rotation photograph; a positive print of the *x*-ray film, that is shown above, is in good agreement with the original pattern.

of only certain *k* indices but that *diffuse streaks occur for every value of k*. An example of this distribution is shown in Fig. 3.

The Weissenberg method resulted in photographs showing "streaky" reflections. Normal beam equatorial Weissenberg photographs show that the $00l$ reflections are the least "streaky" in character and that all of the $h0l$ reflections are spread out along continuous curves. Indices can be assigned to reflections on the basis of an orthohexagonal unit cell. The dimensions of this cell and of the corresponding hexagonal unit are the following:

Orthohexagonal cell	*Hexagonal cell*
a=66.52 Å (12× 5.54 Å)	a_1=38.40 Å
b=38.40 Å (4× 9.60 Å)	a_2=38.40 Å
c=96.62 Å (8×12.08 Å)	c =96.62 Å

The multiplicity of the sub-unit along the three axes is expected to vary in different samples. This may be similar to the polymorphous forms of mica which show such a variation along the *c* axis, as reported by Hendricks and Jefferson (1939).

The agreement between the calculated and observed interplanar spac-

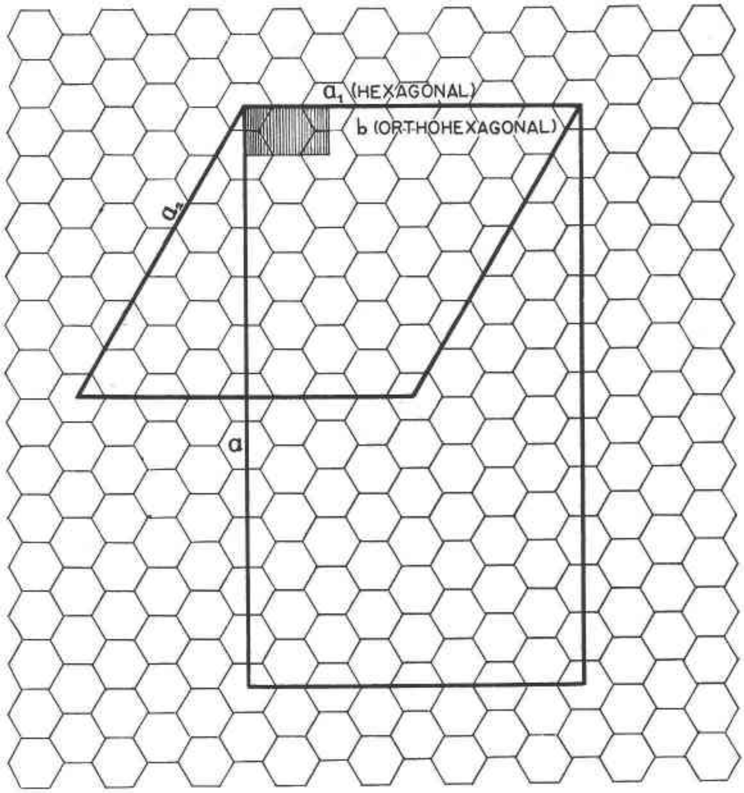

FIG. 4. A possible relationship between the hexagonal a_1 and a_2 and orthohexagonal *a* and *b* cell dimensions of ekmanite and a hexagonal network of atoms similar to the silicon-oxygen hexagons of the layer lattice silicates. The shaded area shows the approximate dimensions of the 00*l* section of the unit cell of talc.

ings confirms: (1) the unit cell dimensions, (2) the multiplicity along the axes, and (3) the right choice of axes. The hexagonal unit is based on a rhombic section in the a_1 and a_2 plane. The length of these two axes is the twelfth multiple of 3.2 Å, which is approximately the length of one of the edges of a silicon-oxygen hexagon that characterizes the layer lattice silicates. One possible relationship between the length of the hexagonal a_1 and a_2 and orthohexagonal *a* and *b* cell dimensions and such a hexagonal pattern of atoms is shown in Fig. 4. The *ab* plane of a talc-type unit is shown by the shaded area on the diagram. One may observe the apparent relationship between the talc-type and the ekmanite *a* and *b* unit cell dimensions and the fact that the ekmanite *a* axis is an approximately twelfth multiple of the talc-type *a* axis, and that the *b* axis is a fourth multiple of that of the talc-type sub-unit.

The multiplicity along the *c* axis is also significant. The distribution of the 00*l*, *h*0*l*, *hkl* reflections on the rotation and Weissenberg photographs indicate a *c* unit cell dimension which is fundamentally an 8th multiple of a 12.08 Å sub-unit. The 008 ($d_{008}=12.08$ Å) reflection is the strongest one present on the ekmanite powder photographs; 00*l* reflections were $l=n8$ also appear as very prominent and strong reflections.

Consideration of some of the prominent features of the *x*-ray diagrams led to some tentative conclusions about the basic structural pattern of ekmanite. A structural analysis was not attempted due to the fact that certain reflections could not be indexed with sufficient certainty because of their diffuse, "streaky" character and closely spaced distribution. The following facts, however, appear to be significant: (1) the apparent 8 fold multiplicity of the 12.08 Å sub-unit along the *c* axis, (2) the relationship between the orthohexagonal *a* and *b* axes and a hexagonal network of atoms, and also the apparent relationship between a talc-type sub-unit and the ekmanite *a* and *b* unit cell dimensions, and (3) the analogy in both interplanar spacing and intensity between the 008 reflection ($d_{008}=12.08$ Å) and the corresponding 00*l* reflection of certain layer lattice silicates, especially stilpnomelane ($d=12.1$ Å). The chemical composition, differential thermal analysis data and morphology of ekmanite may also be significant. These data seem to suggest that ekmanite possesses a structure which is essentially a packing of talc-type sheets and interleaved cations with possible variations in the sub-units resulting in the super-lattice. This talc-type sub-unit present in the ekmanite lattice appears to have the following dimensions: $a=5.54$ Å, $b=9.60$ Å and $c=12.08$ Å.

Another aspect of the *x*-ray investigations involves the disorder present in the ekmanite lattice. The diffuse streaks of the Laue photographs have been referred to by some authors as "asterism." This phenomenon has been studied by several investigators, including Hendricks and Jefferson, who have examined this effect in the case of the micas, and also by Hutton and Fankuchen (1938), who have made a comparison between the Laue photographs of stilpnomelane and other layer lattice silicates. Hendricks and Jefferson suggested that the diffuse streaks present on the Laue patterns correspond to continuous curves on the Weissenberg diagrams and that both of them can be explained in terms of reflections showing continuous variation in the *l* index but possessing constant *h* and *k* indices. The *x*-ray patterns of most of the layer lattice silicates show such continuous curves only when $k\neq 3n$. When $k=3n$ reflections are sharp spots that suggest a random displacement of the mica layers along the *b* axis by $nb/3$ increments, where *n* is an integer. Random shifts of the structural layers are not restricted to the micas only; they may also be observed with other layer lattice silicates. Brindley, Oughton and Robinson (1950) have shown rotation photographs of chlorites taken of ordered and disordered single crystals. The disordered sample yielded a rotation photograph on which the diffuse streaks appeared when $k \neq 3n$ and sharp spots when $k=3n$. All of the reflections were sharp spots when the sample had an ordered lattice.

The rotation photograph of ekmanite is different because diffuse streaks occur for every value of k, as is shown in Fig. 3. Accordingly, equatorial Weissenberg photographs taken about the b axis show continuous diffuse streaks for all of the $h0l$ reflections. These results suggest that the displacement of the ekmanite structural layers is different from those of the micas of Hendricks and Jefferson and also from the disordered chlorites of Brindley, Oughton and Robinson. The displacement does not leave the reflections undisturbed where $k=3n$ and, therefore, it cannot be attributed to random shifts of $nb/3$ along the b axis. A random and *irregular* shift of the structural layers along the a and b axes may account for the pattern; this would indicate, however, a different type of disorder than the one that is commonly present in the mica and chlorite structures.

Figure 5 shows three dimensional drawings of the reciprocal lattice of a hypothetical crystal. When the lattice has a perfect order (A) all of the

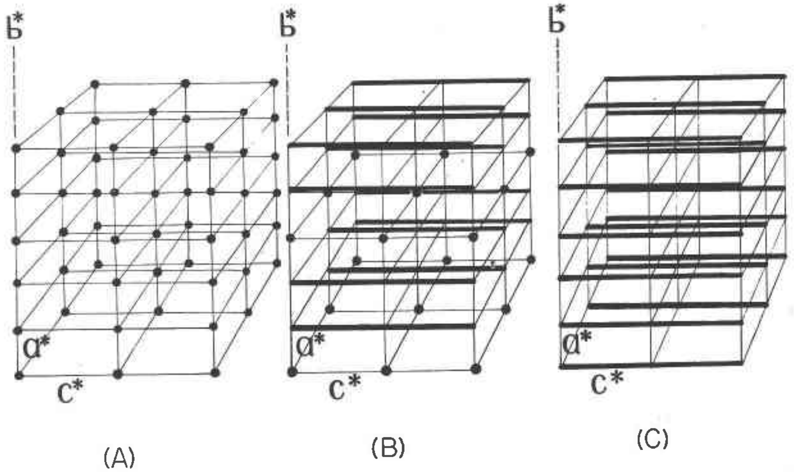

FIG. 5. Three dimensional representations of the reciprocal lattice of a hypothetical crystal: (A) in perfect order, (B) affected by a random displacement of the structural layers by $nb/3$ increments along the b axis, and (C) affected by random and irregular displacement of the structural elements along the a and b axes. The diagram shown in (C) is an exaggerated representation (because it portrays complete disorder) of the effect of random disorder that appears to be present in the ekmanite lattice.

reciprocal lattice points appear as points. A random and regular shift along one axis results in a reciprocal lattice that is essentially a combination of points and straight lines; in case of the displacement by $nb/3$ increments (B) points are found only on those reciprocal lattice planes where $k=3n$. A random and irregular shift of the structural layers along two axes will cause the reciprocal lattice to consist entirely of straight lines (C). The rotation and Weissenberg photographs show related features that may be explained in terms of these examples.

CONCLUSIONS

The results of single crystal x-ray studies and chemical evidence suggest that the lattice of ekmanite is based on talc-type units. Similarity between the structure of ekmanite and of layer lattice silicates of the stilpnomelane type may be anticipated. The multiplicity along all three axes results in a super-lattice that also shows signs of disorder related to random and irregular displacements of the structural layers along the a and b axes. The multiplicity along the a, b and c directions may vary with different samples similar to the polymorphous forms of mica which show such a variation along the c axis. Accordingly a variation of the symmetry of different crystals of ekmanite is anticipated.

ACKNOWLEDGMENT

The author is greatly indebted to Professor W. R. Büssem for his interest and advice.

REFERENCES

BRINDLEY, G. W., OUGHTON, B. M., AND ROBINSON, K. (1950), Polymorphism of the chlorites. I. Ordered structures: *Acta Cryst.*, **3**, 408–416.

DANA, E. S. (1892), Descriptive Mineralogy, John Wiley & Sons, New York, Sixth Edition.

GRUNER, J. W. (1937), Composition and structure of stilpnomelane: *Am. Mineral.*, **22**, 912–925.

GRUNER, J. W. (1944), The structure of stilpnomelane reexamined: *Am. Mineral.*, **29**, 291–298.

HENDRICKS, S. B., AND JEFFERSON, M. E. (1939), Polymorphism of the micas: *Am. Mineral.*, **24**, 729–771.

HUTTON, C. O., AND FANKUCHEN, I. (1938), The stilpnomelane group of minerals: *Mineral. Mag.*, **25**, 172–206.

JAKOB, J. (1923), Zur Kenntnis der Ekmannit-Minerale I.: *Schweiz. Min. Petr. Mitt.*, **3**, 237–239.

Manuscript received July 23, 1953